

UCLA

UCLA Previously Published Works

Title

Heavy eye syndrome versus sagging eye syndrome in high myopia.

Permalink

<https://escholarship.org/uc/item/6k2295fq>

Journal

Journal of American Association for Pediatric Ophthalmology and Strabismus, 19(6)

Authors

Tan, Roland

Demer, Joseph

Publication Date

2015-12-01

DOI

10.1016/j.jaapos.2015.08.012

Peer reviewed



Published in final edited form as:

JAAPOS. 2015 December ; 19(6): 500–506. doi:10.1016/j.jaaapos.2015.08.012.

Heavy eye syndrome versus sagging eye syndrome in high myopia

Roland Joseph D. Tan, MD^a and Joseph L. Demer, MD, PhD^{a,b,c,d}

^aStein Eye Institute, University of California, Los Angeles

^bDepartment of Neurology, University of California, Los Angeles

^cNeuroscience Interdepartmental Program, University of California, Los Angeles

^dBioengineering Interdepartmental Program, University of California, Los Angeles

Abstract

Background—Heavy eye syndrome (HES) presents with esotropia and limited abduction due to superotemporal globe shift relative to the extraocular muscles. Sagging eye syndrome (SES) was originally described in nonmyopic patients exhibiting distance esotropia and cyclovertical strabismus with limited supraduction due to lateral rectus muscle inferodisplacement caused by degeneration of the lateral rectus–superior rectus (LR-SR) band. We hypothesized that SES might also cause strabismus in high myopia.

Methods—Eleven strabismic subjects with high myopia underwent ophthalmological examination and orbital magnetic resonance imaging (MRI) to assess quantitative orbital anatomy.

Results—Of 11 subjects, 5 had HES; 6, SES. Mean axial length in subjects with HES was 32 ± 5 mm; in subjects with SES, 32 ± 6 mm. Average distance esotropia in subjects with HES was 61 ± 39 ; hypotropia was 26 ± 21 . Average distance esotropia in subjects with SES was 23 ± 57 ; hypertropia was 2 ± 2 . All 5 subjects with HES had superotemporal globe prolapse; the LR-SR band was thinned in 6 orbits and ruptured in 2. The mean angle between the lateral rectus and superior rectus muscles in HES was $121^\circ \pm 7^\circ$. In SES the LR-SR band was thinned in 7 orbits and ruptured in 5, with superotemporal soft tissue prolapse. The mean angle between the lateral rectus and superior rectus muscles was $104^\circ \pm 11^\circ$, significantly less than in HES ($P < 0.001$).

Conclusions—SES occurs in highly myopic patients who also exhibit less relative globe dislocation than in HES. Unlike HES, SES exhibits superotemporal soft tissue prolapse that may limit superotemporal globe shift. The distinction is important because surgery for HES uniquely requires creation of a surgical connection between the superior rectus and lateral rectus muscles, whereas SES may be treated with conventional surgery. SES can cause strabismus in high axial myopia. Orbital MRI is useful in differentiating SES from HES.

Correspondence: Joseph L. Demer, MD, PhD, Stein Eye Institute, UCLA, 100 Stein Plaza, Los Angeles, CA 90095-7002 (jld@jsei.ucla.edu).

Publisher's Disclaimer: This is a PDF file of an unedited manuscript that has been accepted for publication. As a service to our customers we are providing this early version of the manuscript. The manuscript will undergo copyediting, typesetting, and review of the resulting proof before it is published in its final citable form. Please note that during the production process errors may be discovered which could affect the content, and all legal disclaimers that apply to the journal pertain.

Progressive esotropia and often hypotropia with limited abduction and supraduction can develop in highly myopic individuals, a condition known as *myopic strabismus fixus*, or heavy eye syndrome (HES).^{1,2} Its pathophysiology was elucidated using orbital computed tomography and magnetic resonance imaging (MRI). Ohta and colleagues³ believed abduction limitation in HES to be caused by weakness of the lateral rectus muscle from its inferior displacement due in turn to its compression by the eyeball against the orbital wall. Krzizok and Schroeder⁴ documented displacements in the paths of all the rectus muscles in HES and particularly noted inferior displacement of the lateral rectus muscle. Yokoyama and colleagues⁵ noted superolateral dislocation of the myopic globe, with displacement of both the superior rectus and lateral rectus muscles; these investigators obtained satisfactory surgical correction by suture anastomosis of the posterior bellies of these two rectus muscles to normalize the relative position of the dislocated myopic globe.⁶⁻⁷

A similar condition in nonmyopic elderly patients was described by Rutar and Demer,⁸ who termed it *sagging eye syndrome* (SES).⁸ Affected individuals commonly develop esotropia for distance viewing—variously termed *age-related distance esotropia*, *divergence paralysis esotropia*, and the like—and/or small-angle hypotropia with decreased supraduction but full abduction. Also present in SES are signs of degenerative adnexal changes such as blepharoptosis and superior sulcus defects.⁸⁻¹⁰ Extensive quantitative MRI studies of SES have been performed, but the studies deliberately excluded patients with high axial myopia in order to avoid confounding interpretation with cases of HES. In SES, high-resolution MRI has demonstrated that the lateral rectus–superior rectus (LR-SR) band, a ligament suspending the lateral rectus pulley, degenerates during aging, producing inferior displacement (“sag”) of the pulley. The medial and inferior rectus pulleys are also displaced inferolaterally in SES, and most rectus muscle paths are elongated and bowed away from the orbital center.^{9,10}

The proposed pathophysiologic mechanisms of HES and SES are not mutually exclusive. Prior exclusion of highly myopic patients from clinical studies of SES was an arbitrary research strategy designed to obtain a homogeneous subject population rather than a diagnostic requirement. We explored the possibility that not all strabismus in highly myopic elderly is due to HES, and that SES, initially described among nonmyopic patients, may occur in them and be treatable with the surgery recommended for SES. We sought to differentiate SES from HES clinically and anatomically.

Subjects and Methods

We reviewed the medical records and high-resolution orbital MRIs of highly myopic adults seen for acquired strabismus at the Jules Stein Eye Institute from 2002 to 2014 who in that interval had enrolled in a prospective study of strabismus. Those with a history of childhood strabismus, strabismus surgery, and other possible causes of ocular movement limitation, such as retinal detachment surgery, abducens nerve palsy, and Duane’s retraction syndrome, were excluded. Participants gave written informed consent according to a protocol approved by the Institutional Review Board of University of California, Los Angeles, and in conformity with the US Health Information Portability and Accountability Act of 1996. All subjects underwent visual acuity assessment, motility examination, slit-lamp and dilated

fundus examination, refraction, and photography of ocular versions. Horizontal and vertical strabismus was measured by prism cover testings at distance and near or with the Krimsky method. Duction limitation was graded from 0 (full movement) to -4 (no movement past the midline).

High-resolution T1- or T2-weighted MRI was performed using a 1.5T scanner (Signa; General Electric, Milwaukee, WI), as previously described.¹² A set of quasicoronal images with 2 mm interval of each orbit, taken perpendicular to the orbital axis (Figure 1) while the involved eye was centrally fixating at a fiber optic target, were used to manually outline cross sections of the extraocular muscles, the globe, and the orbit. The measurements obtained were then analyzed using a normalized, oculocentric coordinate system to identify the pulley locations of participants, based on the horizontal and vertical coordinates relative to the globe center. The data provided by Clark, Miller, and Demer¹² on the normal anterior location of the rectus pulleys were used as a reference to locate the pulleys in the coronal plane.

*ImageJ*¹³ was employed to locate the centroids of the rectus muscles and the globe using quasicoronal images of the orbit 8 mm anterior to the junction of the globe and optic nerve. Lines were drawn connecting the respective muscle centroids to the globe centroids (Figure 2). The resulting angle has been described as the “SR-LR displacement angle.”⁷ The LR-SR band was qualitatively assessed as robust, thinned, or ruptured as previously described.⁹ *ImageJ* was also used to determine globe axial length using axial MRI images.¹⁴ Differences in pulley locations, SR-LR displacement angle, esotropia, and hypotropia were compared using two-tailed Welch *t* test. Pearson’s χ^2 test was used for categorical data comparing limitation in abduction and supraduction. Data are reported as means plus or minus standard deviations.

Results

The 11 highly myopic subjects included in this study were divided into HES and SES groups based on anatomical findings demonstrated on MRI. The HES group comprised 8 orbits of 5 subjects (3 females), of mean age 63 ± 12 years. (Two of the 5 had monocular high myopia; thus, only 8 orbits were included in the HES group.) The SES group comprised 12 orbits of 6 subjects (2 females), of mean age 62 ± 8 years.

MRI of Anatomical Features

On MRI, subjects with HES uniformly exhibited severe superotemporal globe prolapse that displaced the lateral rectus muscle inferiorly and the superior rectus muscle medially (Figure 3A).⁸⁻¹⁰ The LR-SR band in HES was thinned in 6 orbits and ruptured in 2 (Figure 4). The lateral rectus muscle was tightly apposed to the contour of the globe in all orbits with HES.

By contrast, MRI in SES uniformly demonstrated inferior displacement of the lateral rectus muscle and degeneration of the LR-SR band in all subjects (Figure 3B).⁹ No appreciable globe prolapse was noted (Figure 5). The LR-SR band was thinned in 7 orbits and ruptured in 5 orbits with SES. The superotemporal quadrant containing remnants of the degenerated LR-SR band was occupied by lacrimal gland in 2 orbits and orbital fat in 10 orbits.

Rectus Pulley Displacement by MRI

The mean superior rectus pulley in HES was displaced 2.6 mm more medially than in SES ($P < 0.04$, Table 1). The mean inferior rectus pulley location in HES was 0.7 mm more medial than in SES. Both mean superior rectus pulley location and the mean inferior rectus pulley location in HES were 0.2 mm higher than in SES ($P = 0.8$, $P = 0.7$, respectively).

For the horizontal rectus muscles, the mean lateral rectus pulley location in HES was 1.0 mm higher and 1.2 mm more medial than in SES ($P = 0.4$, $P = 0.7$, respectively). The mean medial rectus pulley location in SES was 0.9 mm lower and 0.4 mm more medial than in HES ($P = 0.3$, $P = 0.7$, respectively).

SR-LR Displacement Angle

As defined by Yokoyama and colleagues,⁶ the SR-LR angle was taken as the angle between the line connecting the centroids of the superior rectus muscle and the globe, with the line connecting the centroid of the globe and the lateral rectus muscle (Figure 2). The mean SR-LR angle in HES was $121^\circ \pm 7^\circ$, which was significantly greater than in SES at $104 \pm 11^\circ$ ($P < 0.001$).

Axial Length

Refractive corrections were not informative, because 9 eyes had previously undergone cataract extraction with intraocular lens implantation. Axial MRIs were used to measure the distance between the anterior corneal surface and the anterior retinal surface. The mean axial length for HES was 32 ± 5 mm; for SES, 32 ± 6 mm.

Clinical Findings

HES presents with progressive esotropia, with or without hypotropia, accompanied by limited abduction and/or supraduction.¹⁻⁴ All of our subjects with HES had both esotropia and hypotropia (Table 2). Mean distance esotropia was 61 ± 39 and mean hypotropia was 26 ± 21 . Five eyes with HES had abduction and concurrent supraduction limitation, but the remaining 3 had supraduction limitation only.

SES presents with esotropia and/or small-angle hypotropia associated with limited supraduction but full abduction.⁸⁻¹⁰ Of our subjects with SES, 2 had esotropia with hypotropia, 3 had esotropia only, and 1 had hypotropia only (Table 2). Mean distance esotropia was 23 ± 57 , and mean hypotropia was 2 ± 2 . Eight eyes with SES had limited supraduction with full abduction. The 4 remaining eyes had no duction limitation.

Mean esotropia and hypertropia did not significantly differ statistically between HES and SES ($P = 0.1$, $P = 0.06$, respectively). Mean supraduction limitation was -2.7 in HES, not significantly different from -1.7 in SES ($\chi^2 = 6.7$, $P = 0.25$). Mean abduction limitation was greater in HES (-2.1) compared to none in SES ($\chi^2 = 9.4$, $P < 0.005$). However 3 subjects with HES had no limitation to abduction.

Discussion

Causes of strabismus in highly myopic elderly patients include both HES and SES, but the anatomical relationships of the globe to the extraocular muscles that underlies these two syndromes appear different. Orbital MRI demonstrates inferior lateral rectus displacement and medial superior rectus displacement with severe superotemporal prolapse of the myopic globe in HES,³⁻⁷ whereas only inferior displacement of the lateral rectus results from degeneration of the LR-SR band is seen in SES.⁸⁻¹⁰

In this study, subjects with HES had large-angle distance esotropia averaging $61 \pm 39^\circ$, similar to that observed by Yokoyama and colleagues⁶⁻⁷ ($59 \pm 36^\circ$), as well as mean hypotropia of $26 \pm 21^\circ$, higher than reported by Krzizok and Schroeder⁴ ($10 \pm 11^\circ$). All orbits with HES in the present study had severe superotemporal globe prolapse, inferior displacement of the lateral rectus muscle, and medial displacement of the superior rectus muscle. Notably, the superior rectus pulley location was displaced 2.2 mm medially, whereas the lateral rectus pulley location was displaced 1.5 mm inferiorly in HES, compared to the pulley locations provided by Chaudhuri and Demer⁹ for elderly control subjects (Table 1). The mean SR-LR angle of $121^\circ \pm 7^\circ$ found here for HES is smaller than the value of $180^\circ \pm 31^\circ$ reported by Yokoyama and colleagues.⁶ The lateral rectus muscles of subjects with HES were all tightly apposed to the globe in the current study.

Of the 5 subjects with SES in the current study, 2 had distance paralysis esotropia similar to that of the nonmyopic patients with SES initially described in association with extraocular elongation.⁸⁻¹⁰ Length of the extraocular muscles could not be reliably measured in the current study, because muscle insertions were indistinct from the sclera. The mean distance esotropia of the current subjects was $23 \pm 57^\circ$, exceeding the $11.5 \pm 10.6^\circ$ reported by Chaudhuri and Demer in nonmyopic SES, whereas the mean hypotropia of $2.0 \pm 2.0^\circ$ was smaller than they reported $9.9 \pm 9.4^\circ$.⁹ All cases of SES had inferior lateral rectus muscle displacement as a result of degeneration of the LR-SR bands. Notably, the lateral rectus pulleys in the current study were displaced 1.0 mm inferiorly compared to the pulley locations provided by Chaudhuri and Demer⁹ in their elderly control group (Table 1). No globe prolapse was seen in the current cases of SES despite the presence of high myopia. The displacement angle between the lateral and superior rectus muscles was $104^\circ \pm 11^\circ$ in SES, significantly smaller than the of $121^\circ \pm 7^\circ$ in HES.

The anatomical hallmark of HES is superotemporal prolapse of the myopic globe; no appreciable globe prolapse occurs in SES. Both the superior and lateral rectus muscles in HES are displaced from normal, whereas only the lateral rectus muscle is displaced in SES, resulting in a greater SR-LR displacement angle in HES (Figure 6). While the affected lateral rectus muscle belly is tightly apposed to the prolapsing globe in HES, the it is widely separated from the globe by orbital fat and lacrimal gland in SES.

However, in both HES and SES, the LR-SR bands are either elongated or ruptured. It is clear that degeneration of LR-SR band contributes to the pathology of both conditions. The difference lies in their anatomical etiology, with a superotemporally prolapsing myopic globe in HES and age-related centrifugal displacement of the rectus muscle paths in SES.

We believe that it is clinically prudent to distinguish HES from SES, because this distinction drives the choice of appropriate strabismus surgery. Clinical findings are unlikely to suffice, because there is an overlap of motility findings. Thus, in patients with highly myopic strabismus, we recommend that preoperative orbital imaging be obtained. HES responds to surgical union of the superior rectus and lateral rectus muscle bellies, as initially described by Yokoyama⁶ and can be augmented by medial rectus muscle or inferior rectus muscle recession.¹⁶ A more conventional approach, such as augmented medial rectus muscle recession, is appropriate for highly myopic patients with SES.⁷

Acknowledgments

This study was funded by National Eye Institute Grant EY08313 and an unrestricted grant from Research to Prevent Blindness. MRI surface coils used in imaging are not FDA approved for this purpose.

References

1. Sturn V, Menke MN, Chaloupka K, Landau K. Surgical treatment of myopic strabismus fixus: a graded approach. *Graefes Arch Clin Exp Ophthalmol*. 2008; 246:1323–1329. [PubMed: 18597103]
2. Ward DM. The heavy eye phenomenon. *Trans Ophthalmol Soc UK*. 1967; 87:717–726. [PubMed: 5255254]
3. Ohta M, Iwashige H, Hayashi T, Maruo T. Computed tomography findings in convergent strabismus fixus. *Nippon Ganka Gakkai Zasshi Soc*. 1995; 99:980–985.
4. Krzizok TH, Schroeder BU. Measurement of recti eye muscle paths by magnetic resonance imaging in highly myopic and normal subjects. *Invest Ophthalmol Vis Sci*. 1999; 40:2554–2560. [PubMed: 10509649]
5. Yamaguchi M, Yokoyama T, Shiraki K. Surgical procedure for correcting globe dislocation in highly myopic strabismus. *Am J Ophthalmol*. 2009; 149:341.e2–346.e2. [PubMed: 19939345]
6. Yokoyama, T.; Ataka, S.; Tabuchi, H.; Shiraki, K.; Miki, T. Treatment of progressive esotropia caused by high myopia—a new surgical procedure based on its pathogenesis. In: de Faber, J-T., editor. *Transactions: 27th Meeting, European Strabismological Association, Florence, Italy, 2001*. Lisse, Netherlands: Swets & Zeitlinger, Lisse; 2002. p. 145-148.
7. Yamada M, Taniguchi S, Muroi T. Rectus eye muscle paths after surgical correction of convergent strabismus fixus. *Am J Ophthalmol*. 2002; 134:630–632. [PubMed: 12383836]
8. Rutar T, Demer JL. “Heavy eye” syndrome in the absence of high myopia: a connective tissue degeneration in elderly strabismic patients. *J AAPOS*. 2009; 13:36–44. [PubMed: 18930668]
9. Chaudhuri Z, Demer JL. Sagging eye syndrome connective tissue involution as a cause of horizontal and vertical strabismus in older patients. *JAMA Ophthalmol*. 2013; 131:619–625. [PubMed: 23471194]
10. Demer JL. Connective tissues reflect different mechanisms of strabismus over the life span: The Apt Lecture. *J AAPOS*. 2004; 18:309–315. [PubMed: 25173891]
11. Clark RA, Demer JL. Effect of aging on human rectus extraocular muscle paths demonstrated by magnetic resonance imaging. *Am J Ophthalmol*. 2002; 34:872–878. [PubMed: 12470756]
12. Clark RA, Miller JM, Demer JL. Three dimensional location of human rectus pulleys by path inflections in secondary gaze positions. *Invest Ophthalmol Vis Sci*. 2000; 41:3787–3797. [PubMed: 11053278]
13. Rasband, WS. ImageJ. Bethesda, MD: US National Institutes of Health; 1997–2014. <http://imagej.nih.gov/ij/>
14. Bencic G, Vatavuk Z, Marotti M, et al. Comparison of A-scan and MRI for the measurement of axial length in silicone oil-filled eyes. *Br J Ophthalmol*. 2009; 93:502–505. [PubMed: 19074920]
15. Krzizok TH, Kaufmann H, Traupe H. Elucidation of restrictive motility in high myopia by magnetic resonance imaging. *Arch Ophthalmol*. 1997; 115:1019–1027. [PubMed: 9258224]

16. Leo SW, Del Monte M. Surgical correction of myopic strabismus fixus by modified loop transposition with scleral myopexy. *J AAPOS*. 2007; 11:95.

Author Manuscript

Author Manuscript

Author Manuscript

Author Manuscript

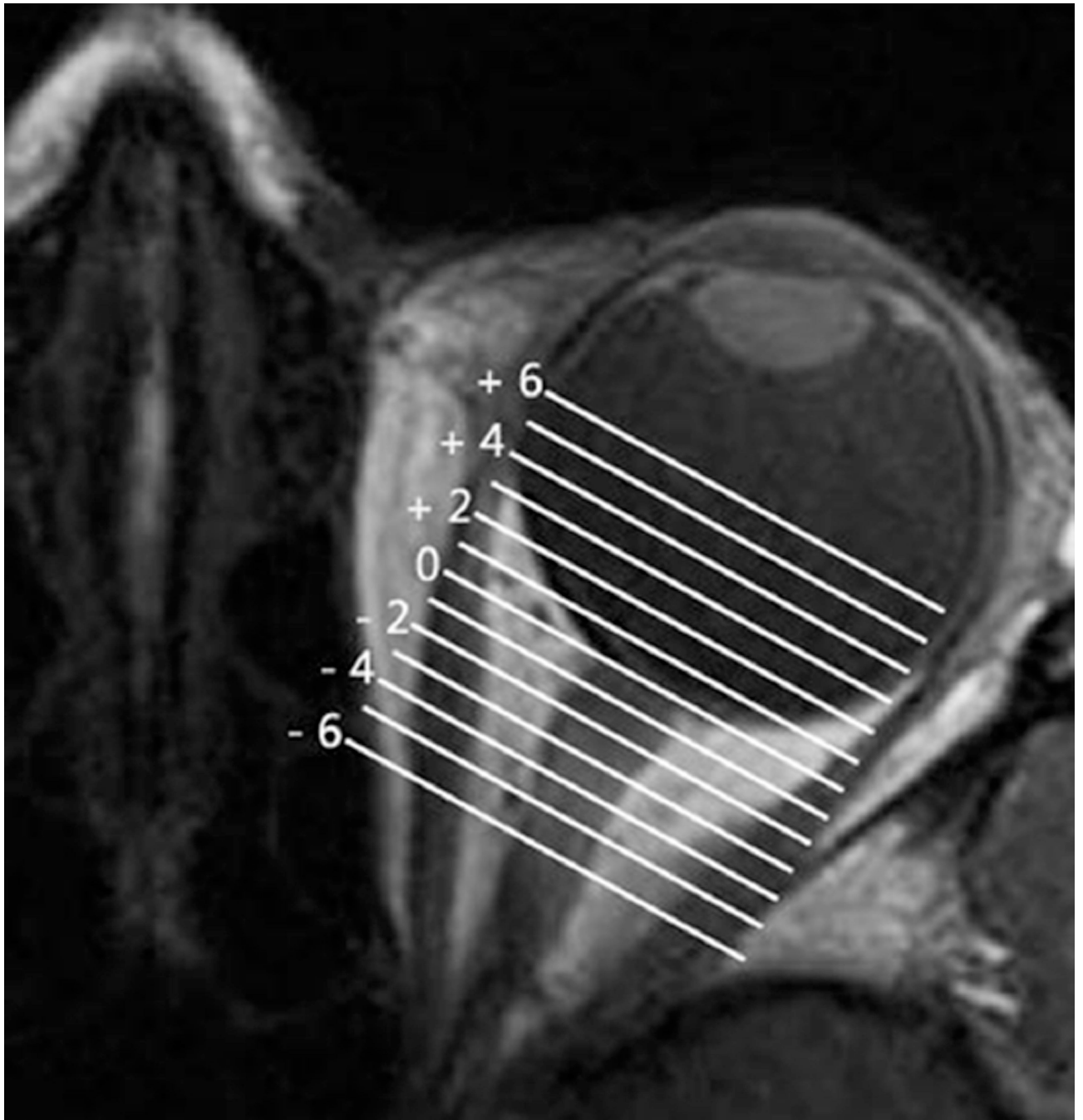


FIG 1. Gadodiamide-enhanced, T1-weighted axial magnetic resonance image (MRI) of the left eye of a normal subject in central gaze that serves as a reference for the quasicoronal images shown in the subsequent figures. Plane 0 contains the optic nerve-globe junction.

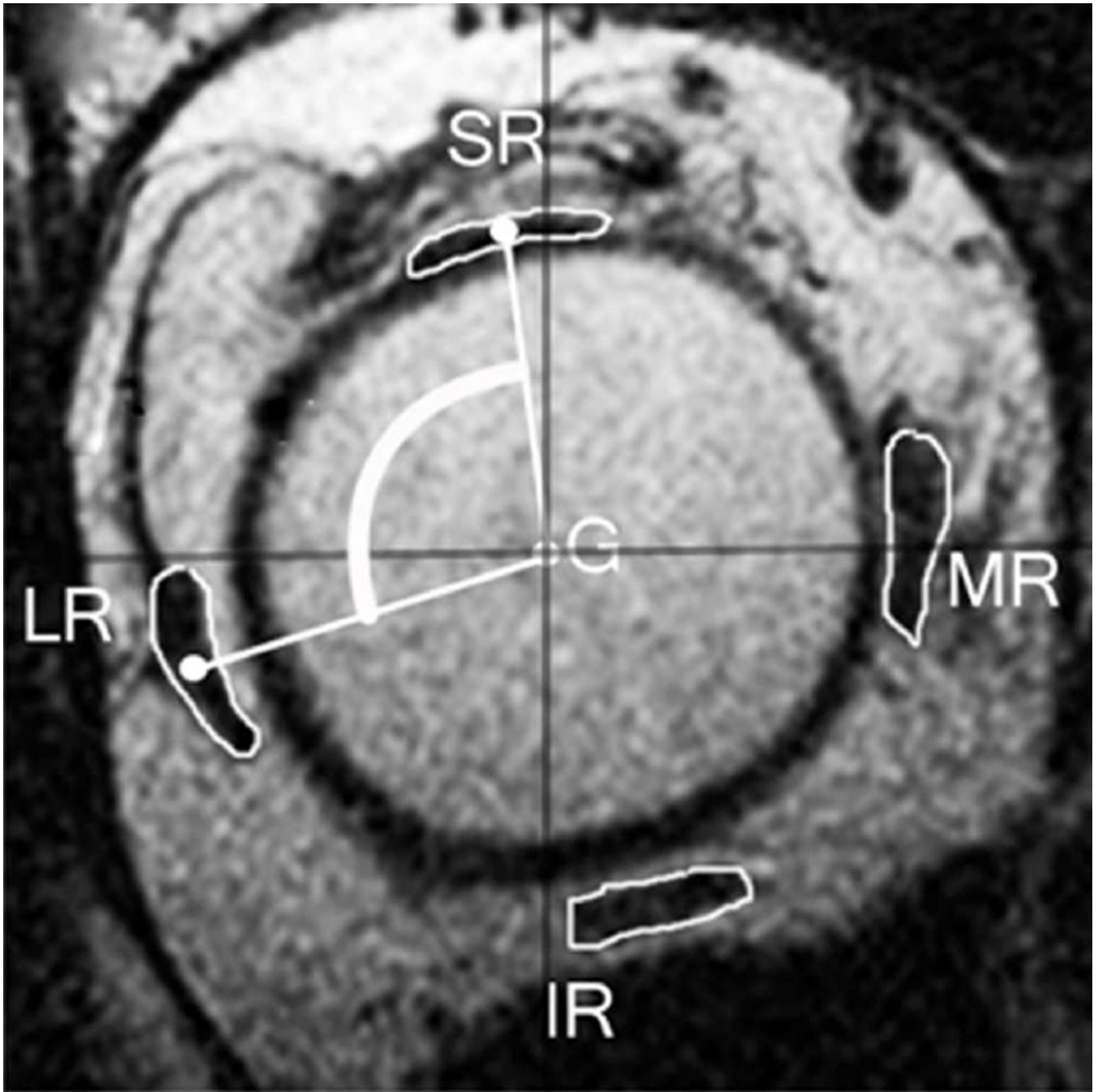


FIG 2.

Quasicoronal, T2-weighted MRI of the right orbit of subject 6, 8 mm from the globe– optic nerve junction illustrating the superior rectus–lateral rectus angle (white arc), measured at 101° , formed by lines connecting the centroids (white dots) of the superior rectus (SR) muscle and globe (G) with that connecting the centroids of the globe and the lateral rectus (LR) muscle. MR, medial rectus muscle; IR, inferior rectus muscle.

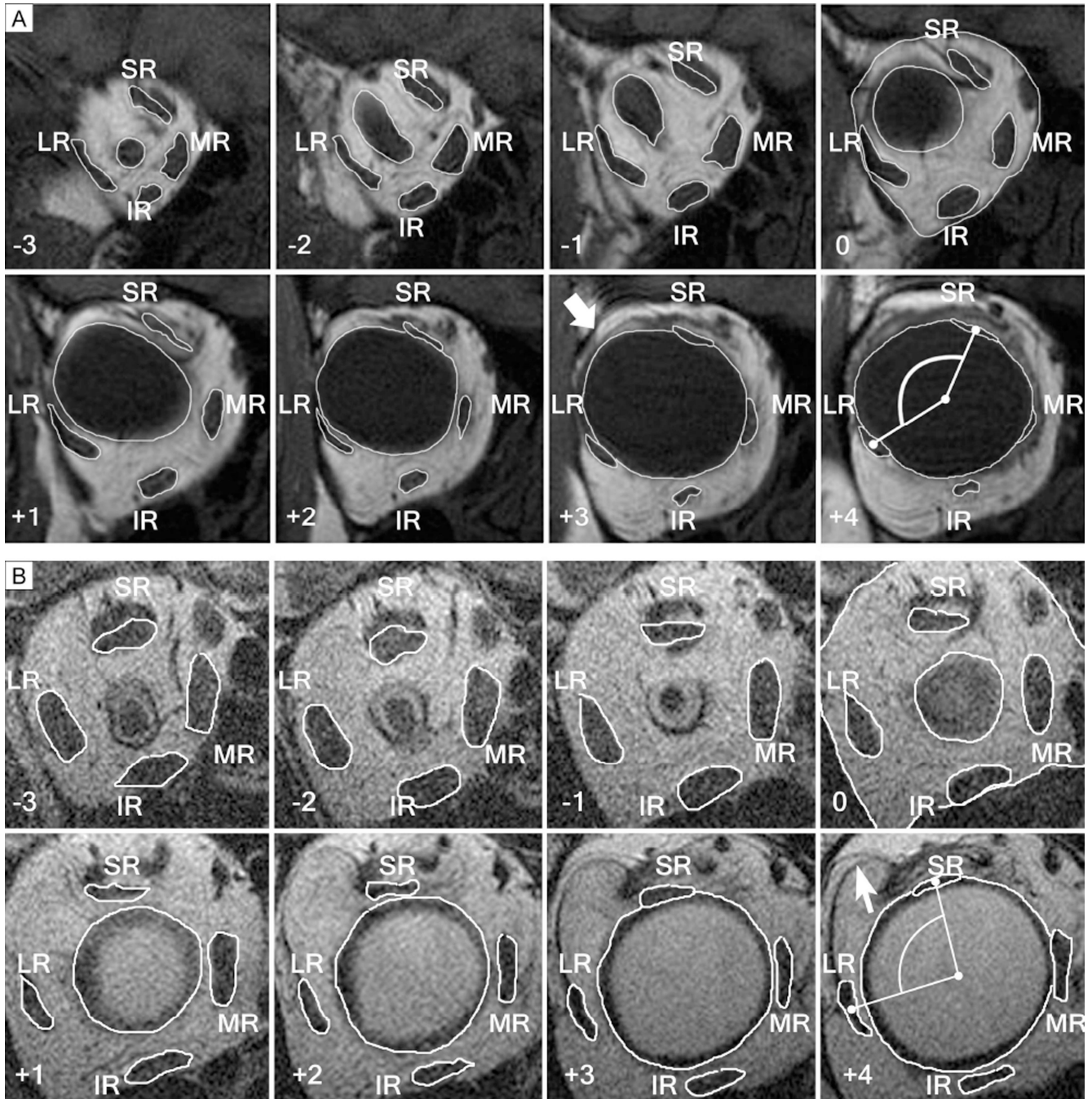


FIG 3. Quasicausal MRI at 2 mm intervals in central gaze, arranged from posterior at upper left to anterior at lower right. Image planes defined as in Figure 1, abbreviations as defined in Figure 2. A, Heavy eye syndrome (HES) with T1-weighted imaging of the right orbit of subject 2. Superotemporal prolapse (white arrow) is prominent in the equatorial region (planes +1 to +4), leading to inferior displacement of the lateral rectus muscle and medial displacement of the superior rectus muscle. Note tight apposition of the LR muscle to the globe. B, Sagging eye syndrome (SES) in subject 6 with T2-weighted imaging. Globe

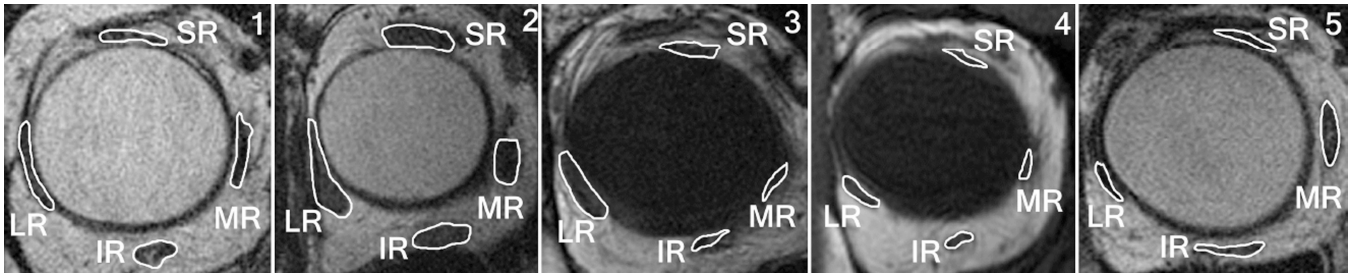
prolapse is absent but there is inferior sag of the lateral rectus muscle due to lateral rectus–superior rectus (LR-SR) band degeneration whose rupture site is indicated by the white arrow. Soft tissue including orbital fat (F) occupies the superotemporal quadrant under the LR-SR band.

Author Manuscript

Author Manuscript

Author Manuscript

Author Manuscript

**FIG 4.**

Quasicoronal MRI of subjects 1 to 5 with HES showing dislocation of the globe superotemporal to the center of the rectus pulley array with inferior displacement of the lateral rectus muscle and medial displacement of the superior rectus muscle. The lateral rectus muscle is tightly apposed to the globe. Left orbits of subjects 2 and 3 are digitally reflected to the right eye orientation for ease of comparison. Abbreviations as in Figure 2.

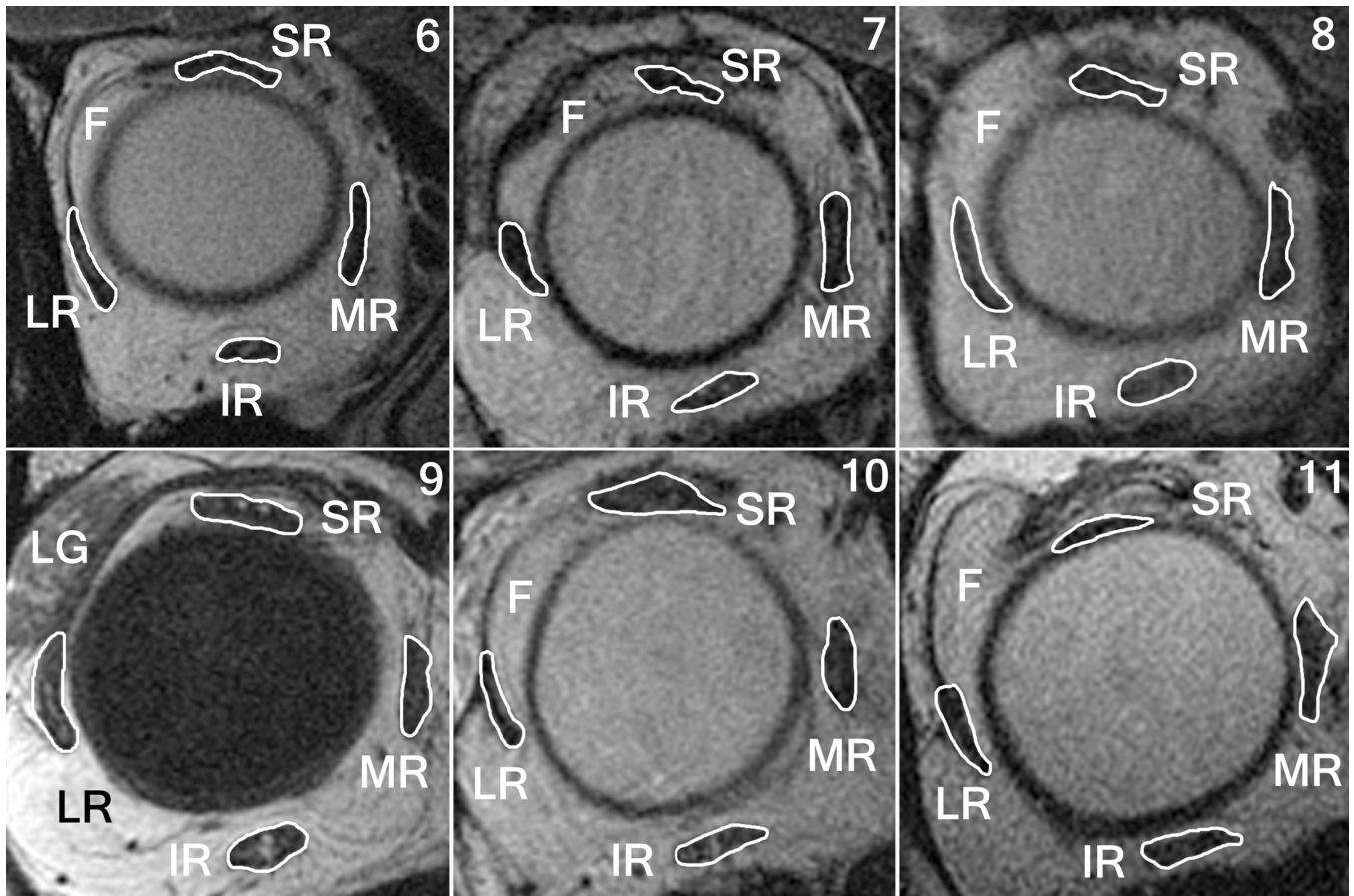


FIG 5. Quasicoronal MRI images of the right orbit of subjects 6 to 11 with SES showing fat (*F*) and lacrimal gland (*LG*) tissues migrating into the superotemporal orbit under the degenerated LR-SR band with inferior displacement of the lateral rectus muscle. The lateral rectus muscle is distracted away from the globe. Imaging is T2-weighted except for subject 9. Abbreviations as in Figure 2.

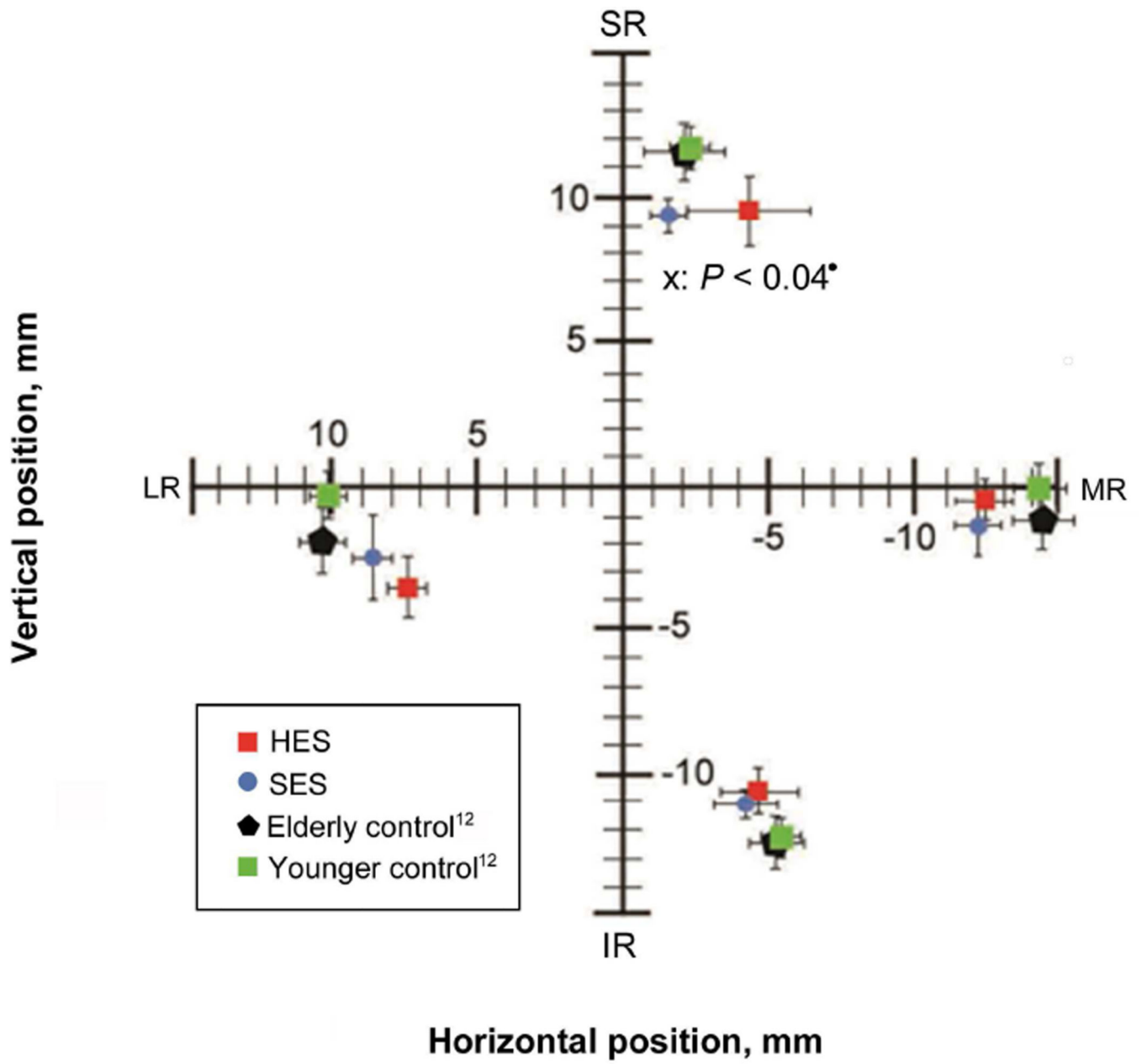


FIG 6. Rectus pulley locations of subjects with heavy eye syndrome, sagging eye syndrome, elderly orthotropic control,⁹ and younger orthotropic control subjects.⁹ Abbreviations as in Figure 2.

Table 1
Clinical presentation of heavy eye syndrome (HES) and sagging eye syndrome (SES)

Subject number	Laterality	Distance esotropia, PD	Distance hypotropia, PD	Abduction deficit	Supraduction deficit
HES					
1	Right Left	45	8	0 0	-2 -1
2	Left	35	25	-4	-4
3	Left	120	60	-4	-4
4	Right Left	25	8	0 -2	-4 -4
5	Right Left	80	30	-4 -4	-2 -1
Mean ± SD		61 ± 39	26 ± 22		
SES					
6	Right Left	18	4	0 0	0 0
7	Right Left	75	0	0 0	-4 -4
8	Right Left	18	4	0 0	-3 -3
9	Right Left	4	0	0 0	0 0
10	Right Left	0	4	0 0	-2 -2
11	Right Left	20	0	0 0	-1 -1
Mean ± SD		23 ± 57	2 ± 2	0	
<i>P</i> value		0.1	0.06	0.05*	0.3

PD, prism diopter; *SD*, standard deviation.

Table 2
Rectus pulley location in heavy eye syndrome (HES) and sagging eye syndrome (SES)

Pulley Coordinate	Medial rectus mm		Superior rectus mm		Lateral rectus mm		Inferior rectus mm	
	Lateral mean	Superior mean	Lateral mean	Superior mean	Lateral mean	Superior Mean	Lateral mean	Superior mean
Elderly control ¹²	-14.5	-1.05	-2.1	11.5	10.1	-2.0	-5.1	-12.6
Young control	-14.4	-0.1	-2.3	11.8	10.1	-0.3	-5.4	-12.2
HES	-12.5	-0.6	-4.3	9.6	7.2	-3.9	-4.8	-10.8
SE	0.56	0.7	1.04	0.54	0.48	0.62	0.8	0.54
SES	-12.1	-1.5	-1.7	9.4	8.4	-2.8	-4.1	-11.0
SE	0.6	0.5	0.4	0.6	0.4	0.7	0.6	0.4
<i>P</i> value	0.7	0.3	0.04*	0.8	0.7	0.4	0.99	0.7

SE, standard error.